

Synthesis and Characterization of New *hypho*-Dithiaborane Clusters: Structural and Bonding Links between Electron-Deficient and Electron-Precise Cage Systems

Sang Ook Kang and Larry G. Sneddon*

Contribution from the Department of Chemistry and Laboratory for Research on the Structure of Matter, University of Pennsylvania, Philadelphia, Pennsylvania 19104-6323.

Received October 17, 1988

Abstract: The dithiaborane anion *hypho*-S₂B₆H₉⁻ (I) was produced in high yield by the reaction of *arachno*-S₂B₇H₈⁻ with excess acetone. Subsequent reaction of I with excess methyl iodide gave *hypho*-2,3-(CH₃)₂-2,3-S₂B₆H₈ (II). A single-crystal X-ray determination of II showed that the compound has an eight-vertex *hypho* cage geometry, which can be derived from an octadecahedron by removing three vertices. Alternatively, II can be considered a dibridged derivative of hexaborane(10). Crystal data for II: space group P2₁/c; Z = 4; a = 5.753 (1), b = 7.293 (1), c = 23.380 (3) Å; β = 92.087 (2)°; V = 980.2 Å³. The structure was refined by full-matrix least squares to a final R of 0.051 and R_w of 0.071 for the 1394 reflections, which had F₀² > 3σ(F₀²). The reaction of I with diiodomethane gave *hypho*-1-CH₂-2,5-S₂B₆H₈ (III) in good yield. A single-crystal X-ray structural determination of III showed that it has a nine-vertex *hypho* cage geometry derived from an icosahedron by removal of three vertices. Furthermore, the cage is observed to have a unique CH₂ unit bridging the two sulfur atoms forming an open five-membered face. Crystal data for III: space group C/c; Z = 4; a = 6.9538 (6), b = 11.850 (2), c = 9.9202 (6) Å; β = 104.689 (6)°; V = 790.7 Å³. The structure was refined by full-matrix least squares to a final R of 0.042 and R_w of 0.055 for the 635 reflections, which had F₀² > 3σ(F₀²). The dithiaborane anion *hypho*-S₂B₇H₁₀⁻ (IV) was produced by the reaction of *hypho*-S₂B₆H₉⁻ with BH₃·THF. Alternatively, IV may be prepared in better yields either by the reaction of *arachno*-S₂B₇H₈⁻ with BH₃·THF or by the direct reaction of *arachno*-6,8-S₂B₇H₉ with NaBH₄. Protonation of IV gives the neutral compound *hypho*-7,8-S₂B₇H₁₁ (V) in good yield. V is isoelectronic with III and, on the basis of the spectroscopic data, is proposed to adopt a similar *hypho* cage geometry in which a BH₂ unit bridges the two sulfur atoms on the five-membered face with an additional hydrogen bridge between the B10 and B11 borons.

Most polyhedral boranes have been found to be members of the *closo*, *nido*, or *arachno* electronic classes, containing $n + 1$, $n + 2$, or $n + 3$ skeletal electron pairs, respectively (where n = the number of cage atoms). Although many exceptions are known, compounds that fall into these classes generally have predictable structures based on closed deltahedra or deltahedra missing one or two vertices, respectively.¹ There are many fewer members of the *hypho* electronic class, that is clusters containing $n + 4$ skeletal electrons. Examples include B₆H₁₀(PMe₃)₂,² B₅H₁₂,³ B₅H₉L₂ (L = NR₃ or PR₃),^{4,5} B₅H₉L (L = dppe, tmeda, etc.),^{6,7} B₃H₅·3PMe₃,^{5b,8} Me₃N-CB₅H₁₁,⁹ B₄H₈·PR₃,¹⁰ B₄H₈·tmeda,¹¹ B₆H₁₄,¹² and B₇H₁₂Fe(CO)₄.¹³ Again, simple electronic counting rules would predict that these compounds should have structures based on deltahedra missing three vertices, but actual structural and bonding patterns in the class have still not been established.

We recently reported¹⁴ that when the *arachno*-S₂B₇H₈⁻ anion is reacted with acetonitrile, reduction of the nitrile and insertion of the resulting imine unit into the cage occurs to yield the 11-vertex *hypho* cluster *hypho*-5-CH₃-5,11,7,14-CNS₂B₇H₈. Structural characterization of this compound demonstrated that, in agreement with its $n + 4$ skeletal electron count, it adopts an open-cage geometry, which may be derived from a 14-vertex bicapped hexagonal antiprism by removal of three vertices. These results suggested that the *arachno*-S₂B₇H₉ cage system might serve as a primary starting material for the syntheses of a wide range of new *hypho* clusters. Furthermore, because of their increased number of skeletal bonding electrons and, as a result, their greater ability to form two-center two-electron, rather than multicenter, interactions, these *hypho* clusters might well exhibit structural and bonding features that bridge those observed in electron-precise and electron-deficient cage systems. We have now investigated these possibilities and report here the syntheses and structural characterizations of a unique series of eight- and nine-vertex dithiaborane clusters having formal *hypho* skeletal electron counts.

Experimental Section

All manipulations were carried out using standard high-vacuum or inert-atmosphere techniques described by Shriver.¹⁵

Materials. *arachno*-6,8-S₂B₇H₉ was prepared as reported previously.¹⁶ Methylene chloride was dried over calcium chloride. Dioxane and tetrahydrofuran were freshly distilled from sodium benzophenone. Acetone was decanted from a saturated sodium iodide solution at room temperature and then cooled at -10 °C to form the crystalline sodium iodide complex. The solid was filtered and then warmed to room temperature. The liberated acetone was then distilled over 4-Å molecular sieves. Borane-tetrahydrofuran, sodium hydride, methyl iodide, diiodomethane, and bis(triphenylphosphoranylidene)ammonium chloride (PPN⁺Cl⁻) were purchased from Aldrich and used as received. Sodium borohydride was obtained from EM Science. Anhydrous hydrogen chloride (Matheson) was purified by vacuum fractionation through a -110 °C trap.

- (1) Wade, K. *Adv. Inorg. Chem. Radiochem.* **1976**, *18*, 1-66.
- (2) Mangion, M.; Hertz, R. K.; Denniston, M. L.; Long, J. R.; Clayton, W. R. Shore, S. G. *J. Am. Chem. Soc.* **1976**, *98*, 449-453.
- (3) Rimmel, R. J.; Johnson, H. D., II; Jaworinsky, I. S.; Shore, S. G. *J. Am. Chem. Soc.* **1975**, *97*, 5395-5403.
- (4) (a) Burg, A. B. *J. Am. Chem. Soc.* **1957**, *79*, 2129-2132. (b) Savory, C. G.; Wallbridge, M. G. H. *J. Chem. Soc., Dalton Trans.* **1973**, 179-184.
- (5) (a) Fratini, A. V.; Sullivan, G. W.; Denniston, M. L.; Hertz, R. K.; Shore, S. G. *J. Am. Chem. Soc.* **1974**, *96*, 3013-3015. (b) Kameda, M.; Kodama, G. *Inorg. Chem.* **1980**, *19*, 2288-2292.
- (6) Alcock, N. W.; Colquhoun, H. M.; Haran, G.; Sawyer, J. F.; Wallbridge, M. G. H. *J. Chem. Soc., Chem. Commun.* **1977**, 368-370.
- (7) Miller, N. E.; Miller, H. C.; Muetterties, E. L. *Inorg. Chem.* **1964**, *3*, 866-869.
- (8) Hertz, R. K.; Denniston, M. L.; Shore, S. G. *Inorg. Chem.* **1978**, *17*, 2673-2674.
- (9) Duben, J.; Heřmánek, S.; Štibr, B. *J. Chem. Soc., Chem. Commun.* **1978**, 287.
- (10) Kodama, G.; Kameda, M. *Inorg. Chem.* **1979**, *18*, 3302-3306.
- (11) (a) Colquhoun, H. M. *J. Chem. Res.* **1978**, 451. (b) Alcock, N. W.; Colquhoun, H. M.; Haran, G.; Sawyer, J. F.; Wallbridge, M. G. H. *J. Chem. Soc., Dalton Trans.* **1982**, 2243-2255.
- (12) Breilochs, B.; Binder, H. *Angew. Chem., Int. Ed. Engl.* **1988**, *27*, 262-263.
- (13) (a) Hollander, O.; Clayton, W. R.; Shore, S. G. *J. Chem. Soc., Chem. Commun.* **1974**, 604-605. (b) Mangion, M.; Clayton, W. R.; Hollander, O.; Shore, S. G. *Inorg. Chem.* **1977**, *16*, 2110-2114.

- (14) Kang, S. O.; Sneddon, L. G. *Inorg. Chem.*, in press.
- (15) Shriver, D. F.; Drezdson, M. A. *The Manipulation of Air Sensitive Compounds*, 2nd ed.; Wiley: New York, 1986.
- (16) Plešek, J.; Heřmánek, S.; Janoušek, Z. *Collect. Czech. Chem. Commun.* **1977**, *42*, 785-792.

Physical Measurements. ^{11}B NMR spectra at 160.5 and 64.2 MHz and ^1H NMR spectra at 500 and 200 MHz were obtained on Bruker AM-500 and Bruker AF-200 spectrometers equipped with appropriate decoupling accessories. All ^{11}B chemical shifts are referenced to $\text{BF}_3\cdot\text{O}(\text{C}_2\text{H}_5)_2$ (0.0 ppm), with a negative sign indicating an upfield shift. All proton chemical shifts were measured relative to internal residual benzene from the lock solvent (99.5%, C_6D_6) and then referenced to Me_4Si (0.0 ppm).

Two-dimensional COSY ^{11}B - ^{11}B NMR experiments¹⁷ were conducted with s-type selection parameters at 160.5 MHz for I and V and 64.2 MHz for II and IV. The sweep widths in the F_2 direction were 25 000 Hz and in the F_1 direction 12 500 Hz for I and V, 5000 and 2500 Hz for II, and 10 000 and 5000 Hz for IV. A total of 256 increments (increment size of 0.04 ms) for I and V, 128 increments (increment size of 0.2 ms) for II, and a total of 128 increments (increment size of 0.1 ms) for IV were collected, each slice having 1K data points. The data were zero-filled once for I and V and twice in the F_1 direction for II and IV. These data were 2D Fourier transformed with sine-bell apodization in both domains. A total of 100 scans was taken for I and V and 200 scans for II and IV, with each increment having a recycling time of 100 ms.

High- and low-resolution mass spectra were obtained on a VG Micromass 7070H mass spectrometer. Infrared spectra were obtained on a Perkin-Elmer 1430 spectrophotometer.

Reaction of *arachno*- $\text{S}_2\text{B}_7\text{H}_8^-$ with Acetone. A solution of $\text{Na}^+\text{S}_2\text{B}_7\text{H}_8^-$ was prepared by the reaction in vacuo of excess NaH (~0.1 g, 4.2 mmol) with *arachno*-6,8- $\text{S}_2\text{B}_7\text{H}_9$ (0.45 g, 3.0 mmol) in THF (~25 mL) at ~-20 °C. After 2 h H_2 evolution had ceased, and the resulting yellow solution was filtered. The solvent was removed in vacuo from the filtrate and acetone (20 mL) added to the dry $\text{Na}^+\text{S}_2\text{B}_7\text{H}_8^-$ salt. Analysis of the reaction mixture by ^{11}B NMR after stirring overnight at room temperature revealed that the starting material had been completely consumed and that resonances characteristic of anion I along with a singlet resonance at 20 ppm (borate) were formed. Next, 15 mL of methylene chloride containing 2.3 g (4.0 mmol) of PPN^+Cl^- was added to the solution. The mixture was stirred for 2 h and then concentrated. Water (~20 mL) was introduced, resulting in the formation of a white precipitate. Recrystallization from methylene chloride and diethyl ether gave 1.62 g (2.4 mmol, 80%) of white crystalline $\text{PPN}^+\text{S}_2\text{B}_6\text{H}_5^-$, mp ~330 °C. Anal. Calcd for $\text{P}_2\text{C}_{36}\text{NS}_2\text{B}_6\text{H}_5$: C, 63.90; H, 5.82; N, 2.07; S, 9.46; B, 9.59. Found: C, 63.96; H, 5.69; N, 2.11; S, 9.16; B, 8.36.

Attempted Protonation of $\text{PPN}^+\text{S}_2\text{B}_6\text{H}_5^-$. A 1.62 g (2.4 mmol) sample of $\text{PPN}^+\text{S}_2\text{B}_6\text{H}_5^-$ was dissolved in ~15 mL of methylene chloride. This solution was maintained at -110 °C while ~15 mmol of anhydrous gaseous HCl was added. After 5 h a detachable U-trap was interposed between the reaction flask and the pump. The noncondensable gas that had been produced was removed, and overnight fractionation of the volatiles through a -20 °C trap allowed gaseous HCl and methylene chloride to pass while 0.08 g (0.5 mmol) of *hypho*-7,8- $\text{S}_2\text{B}_7\text{H}_{11}$ (V) was retained.

Reaction of *hypho*- $\text{S}_2\text{B}_6\text{H}_5^-$ with Methyl Iodide. A 0.45 g (3.0 mmol) sample of *arachno*-6,8- $\text{S}_2\text{B}_7\text{H}_9$ was used to generate a solution of the sodium salt of *hypho*- $\text{S}_2\text{B}_6\text{H}_5^-$ as described above. Acetone was removed in vacuo and ~20 mL of dried THF was condensed into the flask. Methyl iodide (3 mL) was then added dropwise to the reaction mixture at -10 °C. Upon warming to room temperature the solution became turbid, and a white precipitate (NaI) formed upon overnight stirring. The solution was filtered and the filtrate concentrated in vacuo. The oily crude product was washed with three portions of ~30 mL of hexanes and concentrated to give a white crystalline material. Sublimation at 45 °C in vacuo gave 0.18 g (1.1 mmol, 37%) of *hypho*-2,3-(CH_3)₂-2,3- $\text{S}_2\text{B}_6\text{H}_8$ (II), mp 92-93 °C. Exact mass measurement calcd for $^{12}\text{C}_2^{14}\text{H}_{14}^{32}\text{S}_2^{11}\text{B}_6$: 168.1095. Found: 168.1106.

Reaction of *hypho*- $\text{S}_2\text{B}_6\text{H}_5^-$ with Diiodomethane. A 0.45 g (3.0 mmol) sample of *arachno*-6,8- $\text{S}_2\text{B}_7\text{H}_9$ was used to generate a solution of the sodium salt of *hypho*- $\text{S}_2\text{B}_6\text{H}_5^-$ as described above. Acetone was removed in vacuo and ~20 mL of dried THF vacuum transferred to the flask. Diiodomethane (10 mL) was then added dropwise at -10 °C. Upon warming the solution to room temperature a white precipitate formed. After overnight stirring, the solution was filtered, concentrated, and dried in vacuo. The crude product was extracted with three ~30-mL portions of hexanes and concentrated to give a white crystalline material. Vacuum sublimation at 50 °C gave 0.15 g (1.0 mmol, 33%) of *hypho*-1- CH_2 -2,5- $\text{S}_2\text{B}_6\text{H}_8$ (III), mp 105-107 °C. Exact mass measurement calcd for $^{12}\text{C}^1\text{H}_{10}^{32}\text{S}_2^{11}\text{B}_6$: 152.0782. Found: 152.0791.

Syntheses of *hypho*-2,5- $\text{S}_2\text{B}_7\text{H}_{10}^-$ (IV) and *hypho*-2,5- $\text{S}_2\text{B}_7\text{H}_{11}$ (V). **Reaction of *hypho*- $\text{S}_2\text{B}_6\text{H}_5^-$ with $\text{BH}_3\cdot\text{THF}$.** To a 100-mL three-neck round-bottomed flask equipped with a dropping funnel and a nitrogen bubbler was added 1.5 g (2.2 mmol) of $\text{PPN}^+\text{S}_2\text{B}_6\text{H}_5^-$ dissolved in 15 mL of methylene chloride. A 10-mL sample of 1 M $\text{BH}_3\cdot\text{THF}$ was then added dropwise under nitrogen and the solution heated to reflux. After 24 h of reaction, the solution was concentrated and 10 mL of water added, resulting in the formation of a white crystalline precipitate. The precipitate was filtered and recrystallization from methylene chloride and diethyl ether gave 0.40 g (0.58 mmol, 26%) of $\text{PPN}^+\text{S}_2\text{B}_7\text{H}_{10}^-$ (IV), mp ~320 °C. Anal. Calcd for $\text{P}_2\text{C}_{36}\text{NS}_2\text{B}_7\text{H}_{41}$: C, 62.81; H, 5.87; N, 2.03; S, 9.30; B, 10.99. Found: C, 61.64; H, 5.55; N, 2.03; S, 9.03; B, 10.15.

Reaction of *arachno*-6,8- $\text{S}_2\text{B}_7\text{H}_9$ with NaBH_4 . A 100-mL three-neck round-bottomed flask equipped with a reflux condenser and nitrogen bubbler was charged with 0.45 g (3.0 mmol) of freshly sublimed *arachno*-6,8- $\text{S}_2\text{B}_7\text{H}_9$, 0.24 g (6.2 mmol) of vacuum-dried NaBH_4 , and 50 mL of dried dioxane under nitrogen. The reaction mixture was heated at mild reflux whereupon H_2 was evolved. After stirring for 4 h, the formation of the *arachno*- $\text{S}_2\text{B}_7\text{H}_8^-$ ion was observed by ^{11}B NMR. A new anion slowly formed when this solution was refluxed over a period of 1 day, with best results obtained when heating was continued for at least 4 days. The reaction mixture was then chilled to 15 °C, resulting in the formation of a milky slurry. Filtration gave a pale yellow precipitate, which was then dissolved in 10 mL of water. This solution was extracted with two 20-mL portions of diethyl ether and the extract concentrated by vacuum evaporation. The viscous yellow product was suspended in ~30 mL of methylene chloride and 15 mmol of anhydrous gaseous HCl added in vacuo. After 20 min stirring at -115 °C, a tared, detachable U-trap was interposed between the flask containing the reaction mixture and the pump. Fractionation of the volatiles through a -10 °C trap overnight yielded a colorless solid, *hypho*-2,5- $\text{S}_2\text{B}_7\text{H}_{11}$ (V; 0.15 g, 0.99 mmol, 33%), mp 72-74 °C. Exact mass measurement calcd for $^{32}\text{S}_2^{11}\text{H}_{11}^{11}\text{B}_7$: 152.0953. Found: 152.0929.

Reaction of *arachno*- $\text{S}_2\text{B}_7\text{H}_8^-$ with $\text{BH}_3\cdot\text{THF}$. A 100-mL round-bottomed flask fitted with a vacuum stopcock was charged with 0.45 g (3.0 mmol) of *arachno*-6,8- $\text{S}_2\text{B}_7\text{H}_9$, excess NaH (0.17 g, 7.1 mmol), and ~20 mL of tetrahydrofuran. The flask was slowly warmed to room temperature in vacuo whereupon H_2 gas was evolved. After gas evolution ceased (~2 h), the resulting yellow solution was filtered, concentrated, and then transferred to a three-neck flask fitted with a dropping funnel and reflux condenser. Dioxane (~50 mL) was added to the solution, which was then heated to reflux. A 15-mL sample of 1 M solution of $\text{BH}_3\cdot\text{THF}$ was added dropwise and reflux continued for 3 days. The reaction mixture was then chilled to 15 °C, resulting in the formation of a milky slurry. Filtration gave a pale yellow precipitate, which was dissolved in ~10 mL of water. This solution was extracted with diethyl ether (2 × 20 mL) and the extract concentrated in vacuo. The yellow viscous product was suspended in ~30 mL of methylene chloride and 15 mmol of anhydrous gaseous HCl added in vacuo. After 30 min stirring at -115 °C, fractionation through a -10 °C trap gave 0.11 g (0.73 mmol, 24%) of *hypho*-2,5- $\text{S}_2\text{B}_7\text{H}_{11}$ (V).

Reaction of *hypho*-2,5- $\text{S}_2\text{B}_7\text{H}_{11}$ (V) with NaH. A 100-mL round-bottomed flask fitted with a vacuum stopcock was charged with 0.32 g (2.1 mmol) of *hypho*-2,5- $\text{S}_2\text{B}_7\text{H}_{11}$, excess NaH (0.1 g, 4.1 mmol), and ~20 mL of tetrahydrofuran. The flask was then warmed to room temperature. After H_2 evolution ceased, the solution was quickly filtered and mixed with 10 mL of methylene chloride containing 1.7 g (3.0 mmol) of PPN^+Cl^- . After stirring for 2 h the solution was concentrated and 20 mL of water was added. The resulting white precipitate was filtered and then recrystallized from methylene chloride and diethyl ether to give 1.24 g (1.8 mmol) of white crystalline $\text{PPN}^+\text{S}_2\text{B}_7\text{H}_{10}^-$ (IV).

Crystallographic Data for *hypho*-2,3-(CH_3)₂-2,3- $\text{S}_2\text{B}_6\text{H}_8$ (II) and *hypho*-1- CH_2 -2,5- $\text{S}_2\text{B}_6\text{H}_8$ (III). Single crystals of II and III were grown at 0 °C over several days in a glass tube under high vacuum. Suitably sized crystals were mounted inside capillaries under an argon atmosphere and transferred to the diffractometer. In both cases refined cell dimensions and their standard deviations were obtained from least-squares refinement of 25 accurately centered reflections.

Collection and Reduction of the Data. Diffraction data were collected at 295 K on an Enraf-Nonius four-circle CAD-4 diffractometer employing $\text{Cu K}\alpha$ radiation from a highly oriented graphite-crystal monochromator. The raw intensities were corrected for Lorentz and polarization effects using the Enraf-Nonius program START.

Solution and Refinement of the Structures. All calculations were performed on a VAX 11/750 computer using the Enraf-Nonius structure package.¹⁸ The full-matrix least-squares refinement was based on F , and the function minimized was $\sum w(|F_o| - |F_c|)^2$. The weights (w) were taken

(17) (a) Bax, A. *Two-Dimensional Nuclear Magnetic Resonance in Liquids*; Delft University Press: Delft, Holland, 1982. (b) Finster, D. C.; Hutton, W. C.; Grimes, R. N. *J. Am. Chem. Soc.* **1980**, *102*, 400-401. (c) Venable, T. L.; Hutton, W. C.; Grimes, R. N. *J. Am. Chem. Soc.* **1984**, *106*, 29-37.

(18) B. A. Frenz and Associates, Inc., College Station, TX 77840, and Enraf-Nonius, Delft, Holland.

Table I. ^{11}B NMR Data

compd	δ , ppm (J , Hz, assign)	cross peaks
<i>hypko</i> - $\text{S}_2\text{B}_6\text{H}_9^-$ (I) ^{a,b}	7.0 (150; B8,9), -22.2 (dd; 150, ~50; B4,7), -25.2 (dt; 145, ~55; B11), -52.0 (135; B10)	B8,9 ^a -B10 (m), B4,7-B10 (s), B11-B10 (s)
<i>hypko</i> -2,3-(CH ₃) ₂ -2,3- $\text{S}_2\text{B}_6\text{H}_8$ (II) ^{a,c}	-3.8 (160; B8,9), -25.0 (150; B4,7), -40.5 (145; B10), -54.2 (dt; 150, ~65; B11)	B8,9 ^d -B10 (s), B8,9-B11 (m), B4,7-B10 (m), B10-B11 (s)
<i>hypko</i> -1-CH ₂ -2,5- $\text{S}_2\text{B}_6\text{H}_8$ (III) ^{a,c}	-6.1 (160; B7,9), -20.7 (150; B10,11), -36.4 (145; B12), -55.4 (dt; 150, ~65; B8)	
<i>hypko</i> - $\text{S}_2\text{B}_7\text{H}_{10}^-$ (IV) ^{a,b}	-5.8 (t; 120; B1), -6.3 (150; B7,9), -24.2 (150; B10,11), -34.8 (130; B12), -53.7 (dt; 150, ~65; B8)	B7,9 ^d -B12 (s), B7,9-B8 (m), B10,11-B12 (w), B12-B8 (s)
<i>hypko</i> -2,5- $\text{S}_2\text{B}_7\text{H}_{11}$ (V) ^{a,c}	2.6 (dd; 160, ~30; B7,9), -11.5 (t, 130; B1), -22.2 (dd; 145, ~45; B10,11), -23.1 (dt; 175, ~55; B8), -54.6 (155; B12)	B7,9 ^a -B12 (s), B10,11-B12 (s), B8-B12 (w)

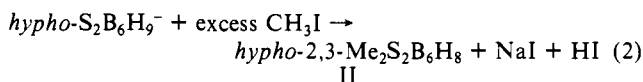
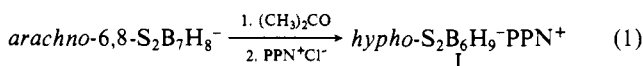
^a 160.5 MHz. ^b CD₂Cl₂ solution. ^c C₆D₆ solution. ^d 64.2 MHz.

as $4F_0^2/\sigma(F_0^2)$ where $|F_0|$ and $|F_c|$ are the observed and calculated structure factor amplitudes. The scattering factors and anomalous dispersion corrections were those stored in the SDP package. Agreement factors are defined as $R = \sum||F_0| - |F_c||/\sum|F_0|$ and $R_w = (\sum w(|F_0| - |F_c|)^2/\sum w|F_0|)^{1/2}$.

Direct methods, using the 11/82 version of MULTAN, yielded the location of all heavy atoms. Anisotropic refinements followed by difference Fourier syntheses resulted in the location of all cage hydrogens in II and all hydrogens in III. Methyl hydrogens of II were calculated using the HYDRO program. The cage hydrogens of II and all hydrogens of III were refined. Final refinements included anisotropic thermal parameters for non-hydrogen atoms and fixed isotropic (6.0) thermal parameters for the hydrogen atoms. The largest residual peaks not in the areas of the heavy atoms in the final difference Fouriers for II and III were 0.25 and 0.14 e/Å³, respectively.

Results

The reaction (eq 1) of the *arachno*- $\text{S}_2\text{B}_7\text{H}_8^-$ anion with excess acetone at room temperature resulted in a cage-degradation reaction, producing a new six-boron anion in excellent yields.



Addition of PPN⁺Cl⁻ to the reaction solution led to the isolation of the PPN salt, which by elemental analysis has the formula PPN⁺[S₂B₆H₉⁻] I. However, it was also found that in situ reaction (eq 2) of the anion with excess methyl iodide results in the good yield formation of the dimethylated derivative, II. Reaction of *hypko*- $\text{S}_2\text{B}_6\text{H}_9^-$ with anhydrous HCl in methylene chloride did not yield the protonated analogue but instead resulted in extensive decomposition and the formation of V, discussed below, in low yields.

Thiaboranes of the formulas $\text{S}_2\text{B}_6\text{H}_9^-$ or (CH₃)₂S₂B₆H₈ would be $n + 4$ hypko skeletal electron systems (8 cage atoms and 12 skeletal electron pairs) and would be expected to adopt open-cage geometries based on an octadecahedron missing three vertices. Possible hypko structures for both I and II that are derived by the removal of one six-coordinate and two five-coordinate vertices are illustrated in Figure 1.

The ^{11}B NMR spectra of I and II (Figure 2) have several similar features and support the structures proposed in Figure 1. Both spectra show four doublets of relative intensities 2:2:1:1, with the resonances at -25.2 ppm in I and -54.2 ppm in II, further split into triplets ($J = \sim 55$ Hz and $J = \sim 65$ Hz, respectively) consistent with their assignment to the boron (B11) in each cage, which is bonded to two bridging hydrogens. The presence of an additional bridge hydrogen in I, located between borons B4 and B7, is indicated by the doublet fine coupling ($J = \sim 50$ Hz) on the intensity two doublets at -22.2 ppm.

The relative chemical shifts of the boron resonances in the spectra of these compounds, and of the analogous resonances arising from the borons in the pyramidal boron fragments of III-V discussed below, are of special interest since they are highly diagnostic of their structures. Thus, I and V exhibit similar spectra and are proposed to have structures in which all of the bridging positions on the pentagonal boron face are occupied. Compounds

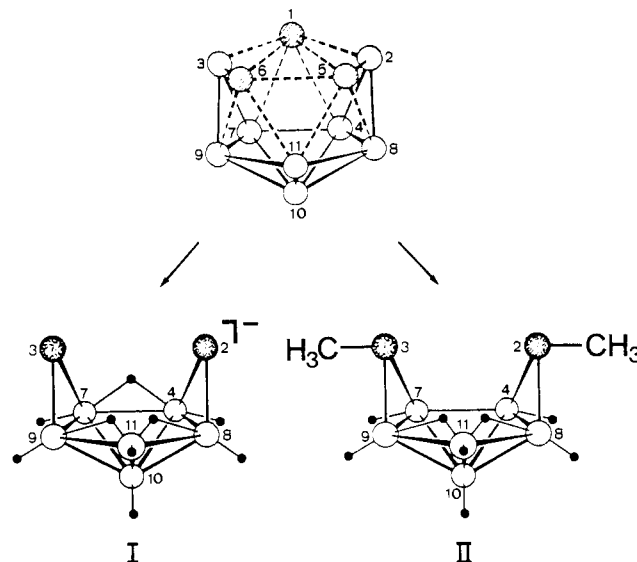


Figure 1. Derivation of eight-vertex hypko structures for I and II from an octadecahedron by removal of three vertices.

Table II. ^1H NMR Data

compd	δ , ppm (assign)
I ^{a,b}	3.56 (BH, 2, $J_{\text{BH}} = 150$ Hz), 1.82 (BH, 2, $J_{\text{BH}} = 145$ Hz), 1.78 (BH, 1, $J_{\text{BH}} = 145$ Hz), 0.64 (BHB, 1, $J_{\text{BHB}} = 45$ Hz), -0.43 (BH, 1, $J_{\text{BH}} = 140$ Hz), -0.97 (BHB, 2)
II ^{c,d}	3.03 (BH), 2.07 (BH), 1.77 (BH), 1.57 (CH ₃), 1.31 (BH), -0.41 (BHB, 2)
III ^{c,d}	3.01 (BH), 2.81 (BH), 1.78 (CH, 1, d, $J_{\text{HH}} = 12$ Hz), 1.47 (CH, 1, d, $J_{\text{HH}} = 12$ Hz), 1.24 (BH), 0.70 (BH), -0.66 (BHB, 2)
IV ^{a,d}	2.53 (BH), 2.18 (BH, d, $J_{\text{HH}} = 8$ Hz), 1.70 (BH, d, $J_{\text{HH}} = 8$ Hz), 1.56 (BH), -0.04 (BH), -0.70 (BHB, 2)
V ^{c,d}	3.03 (BH), 2.56 (BH, m), 2.42 (BH, m), 2.15 (BH, m), 1.45 (BH, d, 8 Hz), -0.47 (BH), ^a -0.47 (BHB, t, 8 Hz), ^e -1.48 (BHB, 2)

^a CD₂Cl₂ solution. ^b 500 MHz. ^c C₆D₆. ^d 200-MHz boron-decoupled proton spectra. ^e Overlapped resonances.

II-IV also exhibit similar spectral features and are each proposed to have structures in which one boron-boron edge is unsubstituted.

The assignments for I and II given in Figure 2, as well as those proposed for III-V, also agree with the 2D ^{11}B - ^{11}B COSY NMR experiments (Table I), which show cross peaks arising from all adjacent borons, except between those borons on the pentagonal face. Since these borons are bridged by either hydrogen^{17b,c} or sulfur atoms,¹⁹ cross peaks are not expected.

The 500-MHz ^1H NMR spectrum of I is shown in Figure 3 and strongly supports the proposed formulation, showing four terminal BH quartets in a relative ratio of 2:2:1:1 and two distinct types of bridging hydrogens in a 1:2 ratio. The bridge resonance at 0.64 ppm also shows septet structure ($J = 45$ Hz) characteristic

Table III. IR Data (cm⁻¹)^a

I	3050 (w), 2960 (w), 2540 (w, sh), 2480 (s), 1980 (w, br), 1585 (m), 1480 (m), 1435 (s), 1370 (w), 1315 (s, sh), 1290 (s), 1260 (s), 1180 (m), 1160 (w), 1115 (s), 1065 (w), 1010 (s), 950 (s), 920 (w), 875 (w), 845 (w), 800 (m), 750 (m), 740 (m), 720 (s), 690 (s), 545 (s), 530 (s), 500 (s), 445 (w), 395 (w)
II	3020 (w), 2960 (w), 2930 (w), 2850 (w), 2560 (s), 2550 (s), 2520 (s), 2500 (s), 1420 (m, br), 1390 (m, br), 1315 (s), 1260 (w), 1100 (w, br), 1010 (m), 995 (m), 975 (m), 935 (w), 875 (w), 850 (w), 810 (w), 720 (w), 705 (w), 660 (w), 610 (w), 550 (w), 520 (w), 505 (w), 410 (w), 360 (w)
III	2970 (w), 2920 (w), 2570 (s), 2550 (s), 2530 (s), 1460 (m, br), 1405 (s), 1195 (w), 1115 (w), 990 (m), 945 (w), 925 (w), 905 (w), 885 (m), 840 (w), 820 (w), 795 (w), 730 (w), 720 (w), 680 (w), 650 (w), 620 (w), 545 (w), 510 (w), 470 (w), 430 (w), 410 (w)
IV	3080 (w), 3060 (w), 2700 (w), 2530 (s), 2420 (m, sh), 2380 (s), 2280 (w), 2220 (w), 2010 (w), 1990 (w), 1965 (w), 1900 (w), 1820 (w), 1770 (w), 1670 (w), 1590 (s), 1480 (s), 1435 (s), 1380 (w), 1320 (s), 1305 (s), 1295 (s), 1270 (s), 1180 (m), 1150 (w), 1115 (s), 1070 (w), 1035 (m), 1025 (w), 995 (s), 925 (w), 875 (w), 845 (w), 790 (w), 745 (s), 720 (s), 690 (s), 615 (w), 535 (s), 500 (s), 450 (w), 390 (m), 350 (w), 315 (w)
V	2570 (s), 2480 (m), 2420 (s), 1980 (w), 1540 (w), 1460 (w), 1140 (m), 1050 (s), 1035 (m, sh), 1005 (s), 975 (w), 960 (w), 915 (w), 870 (m), 835 (w, sh), 825 (m), 765 (w), 735 (w), 660 (w), 640 (w)

^aKBr pellets. s = strong. m = medium. w = weak. sh = shoulder. br = broad.

Table IV. Data Collection and Structure Refinement Information

	II	III
space gp	$P2_1/c$	C/c
<i>a</i> , Å	5.753 (1)	6.9538 (6)
<i>b</i> , Å	7.293 (1)	11.850 (2)
<i>c</i> , Å	23.380 (3)	9.9202 (6)
β , deg	92.087 (2)	104.689 (6)
<i>V</i> , Å ³	980.2	790.7
<i>Z</i>	4	4
ρ (calcd), g cm ⁻³	1.132	1.269
mol formula	C ₂ H ₁₄ B ₆ S ₂	CH ₁₀ B ₆ S ₂
mol wt	167.13	151.08
λ	Cu K α , 1.541 84 Å	Cu K α , 1.541 84 Å
scanning range, deg	4° ≤ 2 θ ≤ 130°	4° ≤ 2 θ ≤ 130°
scan mode	ω -2 θ	ω -2 θ
$\pm h, \pm k, \pm l$, collid	6,8,±27	±8,13,11
no. of measured <i>I</i> 's	1664	671
no. of $F_o^2 > 3\sigma(F_o^2)$	1394	635
no. of variables	116	111
<i>R</i>	0.051	0.042
<i>R_w</i>	0.071	0.055

Table V. Atomic Position Parameters and Their Estimated Standard Deviations for *hypho*-2,3-(CH₃)₂-2,3-S₂B₆H₈ (II)

atom	<i>x</i>	<i>y</i>	<i>z</i>	<i>B</i> , Å ²
S2	0.2799 (2)	-0.1851 (1)	0.90331 (4)	4.85 (2)
S3	0.2881 (1)	0.0172 (1)	0.77545 (4)	4.51 (2)
B4	0.0238 (7)	-0.0242 (6)	0.8844 (2)	4.34 (8)
B7	0.0267 (6)	0.0769 (6)	0.8208 (2)	4.16 (8)
B8	0.2777 (7)	0.0640 (7)	0.9304 (2)	4.65 (9)
B9	0.2836 (6)	0.2382 (7)	0.8198 (2)	4.38 (9)
B10	0.1277 (6)	0.2092 (6)	0.8826 (2)	4.04 (8)
B11	0.4264 (7)	0.2464 (7)	0.8913 (2)	4.64 (9)
C2	0.1880 (9)	-0.3055 (7)	0.9660 (2)	6.6 (1)
C3	0.2172 (7)	0.1057 (6)	0.7045 (2)	5.47 (9)
H4	-0.126 (8)	-0.059 (7)	0.909 (2)	6.0
H7	-0.117 (8)	0.120 (7)	0.796 (2)	6.0
H8	0.282 (8)	0.079 (7)	0.972 (2)	6.0
H9	0.287 (8)	0.360 (7)	0.797 (2)	6.0
H10	0.012 (8)	0.317 (7)	0.897 (2)	6.0
H11	0.479 (8)	0.372 (7)	0.912 (2)	6.0
H811	0.502 (8)	0.112 (7)	0.916 (2)	6.0
H911	0.513 (8)	0.229 (7)	0.846 (2)	6.0

^aAnisotropically refined atoms are given in the form of the isotropic equivalent displacement parameter defined as $\frac{1}{3}[a^2B(1,1) + b^2B(2,2) + c^2B(3,3) + ab(\cos \gamma)B(1,2) + ac(\cos \beta)B(1,3) + bc(\cos \alpha)B(2,3)]$.

of a bridge hydrogen located between two equivalent boron atoms (B4 and B7). Upon boron decoupling this resonance collapses to a triplet ($J = 18$ Hz) arising from coupling to the two terminal hydrogens attached to B4 and B7. The ¹H NMR spectrum of II (Table 11) shows, in addition to the methyl singlet peak, only one bridging hydrogen resonance.

As shown in the ORTEP drawing given in Figure 4, a single-crystal X-ray structural determination of II confirms that the complex adopts a structure similar to the predicted *hypho* geometry in Figure 1. The only previously reported¹³ example of an eight-vertex *hypho* polyhedral borane cage is the ferraborane

Table VI. Interatomic Distances (Å) for II

bond	distances	bond	distances
S2-B4	1.923 (4)	B10-B11	1.744 (5)
S2-B8	1.924 (5)	S2-C2	1.805 (5)
S3-B7	1.921 (4)	S3-C3	1.813 (4)
S3-B9	1.918 (5)	B4-H4	1.08 (5)
B4-B7	1.660 (6)	B7-H7	1.05 (5)
B4-B8	1.895 (6)	B8-H8	0.99 (5)
B4-B10	1.805 (6)	B8-H811	1.39 (5)
B7-B9	1.890 (6)	B9-H9	1.04 (5)
B7-B10	1.815 (6)	B9-H911	1.44 (5)
B8-B10	1.746 (6)	B10-H10	1.09 (5)
B8-B11	1.843 (7)	B11-H11	1.08 (5)
B9-B10	1.761 (6)	B11-H811	1.22 (5)
B9-B11	1.837 (6)	B11-H911	1.19 (5)

Table VII. Bond Angles (deg) for II

bond	angles	bond	angles
B4-S2-B8	59.0 (2)	B7-B9-B10	59.5 (2)
B7-S3-B9	59.0 (2)	B7-B9-B11	109.4 (3)
B2-B4-B7	116.4 (3)	B10-B9-B11	58.0 (2)
S2-B4-B8	60.5 (2)	B4-B10-B7	54.6 (2)
S2-B4-B10	109.2 (2)	B4-B10-B8	64.5 (2)
B7-B4-B8	109.0 (3)	B4-B10-B9	108.2 (3)
B7-B4-B10	63.0 (3)	B4-B10-B11	118.0 (3)
B8-B4-B10	56.2 (2)	B7-B10-B8	108.9 (3)
S3-B7-B4	115.3 (3)	B7-B10-B9	63.8 (2)
S3-B7-B9	60.4 (2)	B7-B10-B11	117.5 (3)
S3-B7-B10	109.0 (2)	B8-B10-B9	110.7 (3)
B4-B7-B9	108.7 (3)	B8-B10-B11	63.7 (2)
B4-B7-B10	62.4 (2)	B9-B10-B11	63.2 (2)
B9-B7-B10	56.7 (2)	B8-B11-B9	103.2 (3)
S2-B8-B4	60.4 (2)	B8-B11-B10	58.2 (2)
S2-B8-B10	111.7 (3)	B9-B11-B10	58.8 (2)
S2-B8-B11	120.6 (3)	B4-S2-C2	103.8 (2)
B4-B8-B10	59.3 (2)	B8-S2-C2	100.7 (2)
B4-B8-B11	109.0 (3)	B7-S3-C3	105.7 (2)
B10-B8-B11	58.1 (2)	B9-S3-C3	100.9 (2)
S3-B9-B7	60.6 (2)	B8-H811-B11	90. (3)
S3-B9-B10	111.5 (3)	B9-H911-B11	88. (3)
S3-B9-B11	120.3 (3)		

anion [Fe(CO)₄B₇H₁₂]⁻. An X-ray crystallographic study showed that the complex has a structure similar to that observed for II, consisting of a B₆H₆ pentagonal-pyramid framework having three bridging hydrogens, as well as BH₃ and Fe(CO)₄ groups bridging nonadjacent boron-boron sites on the face. Thus, both I and II may also be considered as dibridged derivatives of hexaborane(10).

In II the sulfur atoms occupy nonadjacent positions on the face of a B₆H₆ fragment, with the sulfur-sulfur distance (3.34 Å) being too great to allow any direct bonding interaction between these atoms. The boron-sulfur distances (av 1.92 Å) are typical of those observed in polyhedral thiaaboranes.²⁰ The S3-B9-B7 and S2-

(20) (a) Guggenberger, L. J. *J. Organomet. Chem.* **1974**, *81*, 271-280. (b) Pretzer, W. R.; Hilty, T. K.; Rudolph, R. W. *Inorg. Chem.* **1975**, *14*, 2459-2462. (c) Hilty, T. K.; Rudolph, R. W. *Inorg. Chem.* **1979**, *18*, 1106-1108.

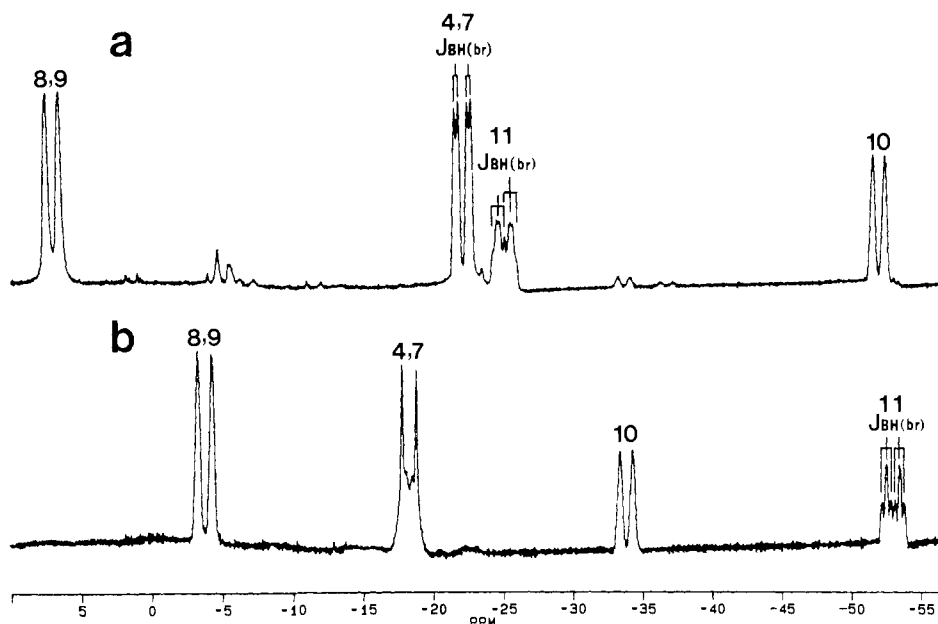


Figure 2. 160.5-MHz ^{11}B NMR spectra of I (a) and II (b).

Table VIII. Atomic Position Parameters and Their Estimated Standard Deviations for *hypko*-1- CH_2 -2,5- $\text{S}_2\text{B}_6\text{H}_8$ (III)

atom	x	y	z	$B, \text{\AA}^2$
S2	1.3645 (3)	0.2423 (1)	0.6052 (2)	5.09 (3)
S5	1.015	0.2008 (1)	0.730	4.86 (3)
B7	1.246 (1)	0.3841 (6)	0.5386 (7)	4.5 (1)
B8	0.975 (1)	0.3953 (6)	0.4949 (9)	5.1 (2)
B9	0.920 (1)	0.3453 (6)	0.6537 (9)	5.1 (2)
B10	1.154 (1)	0.3378 (6)	0.7979 (7)	4.0 (1)
B11	1.3431 (9)	0.3605 (6)	0.7300 (7)	4.0 (1)
B12	1.1196 (9)	0.4377 (5)	0.6588 (7)	3.7 (1)
C1	1.163 (1)	1.1507 (5)	0.6137 (7)	5.3 (2)
H7	1.33 (1)	0.419 (8)	0.488 (9)	6.0
H8	0.90 (1)	0.459 (7)	0.438 (8)	6.0
H9	0.78 (1)	0.359 (7)	0.672 (8)	6.0
H10	1.14 (1)	0.354 (8)	0.904 (7)	6.0
H11	1.48 (1)	0.403 (8)	0.776 (8)	6.0
H12	1.11 (1)	0.542 (7)	0.680 (9)	6.0
H78	1.08 (1)	0.343 (7)	0.438 (9)	6.0
H89	0.87 (1)	0.328 (8)	0.519 (8)	6.0
H1A	1.24 (1)	0.082 (7)	0.658 (8)	6.0
H1B	1.07 (1)	0.154 (7)	0.519 (8)	6.0

^a Anisotropically refined atoms are given in the form of the isotropic equivalent displacement parameter defined as $\frac{1}{3}[a^2B(1,1) + b^2B(2,2) + c^2B(3,3) + ab(\cos \gamma)B(1,2) + ac(\cos \beta)B(1,3) + bc(\cos \alpha)B(2,3)]$.

Table IX. Interatomic Distances (\AA) for III

bond	distances	bond	distances
S2-B7	1.913 (7)	S2-C1	1.789 (8)
S2-B11	1.900 (7)	S5-C1	1.834 (8)
S5-B9	1.922 (8)	B7-H7	1.0 (1)
S5-B10	1.923 (7)	B7-H78	1.40 (8)
B7-B8	1.83 (1)	B10-H10	1.10 (8)
B7-B11	1.867 (9)	B11-H11	1.08 (8)
B7-B12	1.77 (1)	B12-H12	1.26 (8)
B10-B11	1.64 (1)	B8-H8	1.01 (8)
B10-B12	1.788 (9)	B8-H78	1.2 (1)
B11-B12	1.787 (9)	B8-H89	1.17 (9)
B8-B9	1.81 (1)	B9-H9	1.06 (9)
B8-B12	1.75 (1)	B9-H89	1.31 (8)
B9-B10	1.877 (9)	C1-H1A	1.00 (9)
B9-B12	1.76 (1)	C1-H1B	1.01 (7)

B4-B8 planes are bent away from each other and both form dihedral angles of 109° with the pentagonal boron plane. The carbon-sulfur distances in the methanethiol groups are normal, and the C-S-Mp (Mp = midpoint of the B7-B9 and B4-B8 bonds) have bond angles of 105.3° and 104.1° , respectively.

Table X. Bond Angles (deg) for III

bond	angles	bond	angles
B7-S2-B11	58.6 (3)	S2-B11-B10	110.4 (4)
B9-S5-B10	58.5 (3)	S2-B11-B12	108.9 (4)
S2-B7-B8	118.2 (5)	B7-B11-B10	108.8 (4)
S2-B7-B11	60.3 (3)	B7-B11-B12	57.9 (4)
S2-B7-B12	109.0 (4)	B10-B11-B12	62.6 (4)
B8-B7-B11	109.6 (5)	B7-B12-B8	62.6 (4)
B8-B7-B12	58.3 (4)	B7-B12-B9	106.3 (5)
B11-B7-B12	58.8 (4)	B7-B12-B10	106.9 (5)
B7-B8-B9	101.7 (5)	B7-B12-B11	63.3 (4)
B7-B8-B12	59.2 (4)	B8-B12-B9	62.1 (5)
B9-B8-B12	59.0 (4)	B8-B12-B10	117.4 (5)
S5-B9-B8	120.6 (5)	B8-B12-B11	117.1 (5)
S5-B9-B10	60.8 (3)	B9-B12-B10	63.9 (4)
S5-B9-B12	110.8 (4)	B9-B12-B11	107.1 (5)
B8-B9-B10	110.1 (5)	B10-B12-B11	54.8 (4)
B8-B9-B12	58.8 (4)	B7-S2-C1	106.1 (3)
B10-B9-B12	58.8 (4)	B11-S2-C1	103.0 (3)
S5-B10-B9	60.7 (3)	B9-S5-C1	103.3 (3)
S5-B10-B11	112.3 (4)	B10-S5-C1	100.3 (3)
S5-B10-B12	109.4 (4)	S2-C1-S5	113.9 (3)
B9-B10-B11	108.0 (5)	B7-H78-B8	89. (5)
B9-B10-B12	57.3 (4)	B8-H89-B9	94. (5)
B11-B10-B12	62.6 (4)	H1A-C1-H1B	126. (7)
S2-B11-B7	61.0 (3)		

In hexaborane(10), four of the basal edges are bridged by hydrogen atoms, with the fifth unbridged edge exhibiting a boron-boron distance of $1.596(12) \text{\AA}$.²¹ This is, in fact, the shortest boron-boron distance known and is thought to indicate substantial single-bond character.²¹ In II the distance between the unbridged borons B7 and B4 is larger $1.660(6) \text{\AA}$, although still smaller than that normally observed between borons involved in three-center bonding.²²

The two bridging hydrogens in II are located in adjacent bridging positions on the opposite side of the cage from the unbridged site. These hydrogens (HB811 and HB911) are asymmetrically bound, being closer to B11 ($1.22(5)$ and $1.19(5) \text{\AA}$) than to B8 ($1.39(5) \text{\AA}$) and B9 ($1.44(5) \text{\AA}$). This preference agrees with the strong coupling observed in the ^{11}B NMR spectrum between these hydrogens and B11.

(21) Hirshfeld, F. L.; Eriks, K.; Dickerson, R. E.; Lippert, E. L., Jr.; Lipscomb, W. N. *J. Chem. Phys.* **1958**, *28*, 56-61.

(22) Beaudet, R. A. In *Advances in Boron and the Boranes*; Liebman, J. F., Greenberg, A., Williams, R. E., Ed.; VCH Publishers: New York, 1988; pp 417-516.

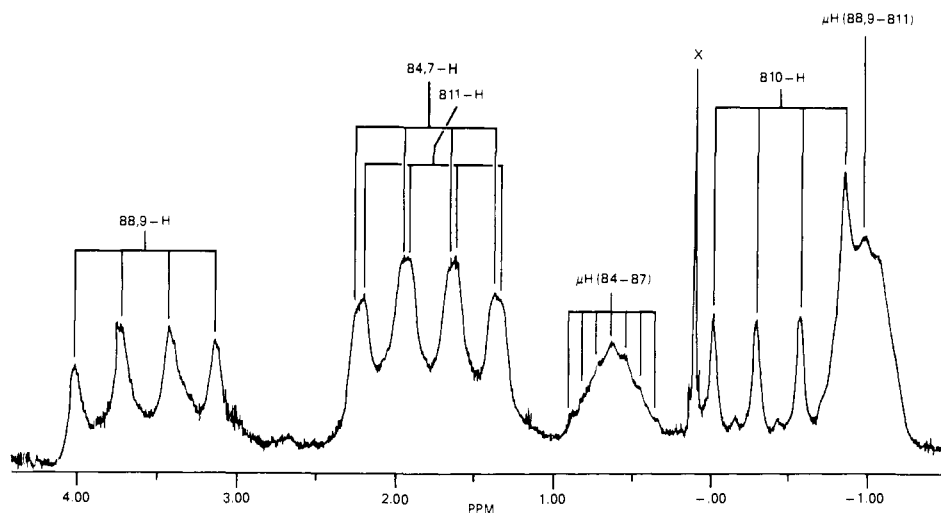


Figure 3. 500-MHz ^1H NMR spectrum of I.

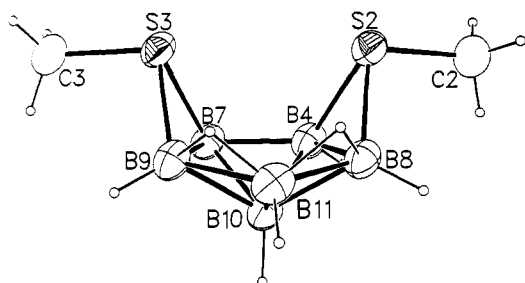
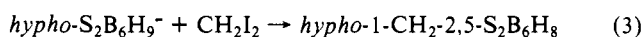


Figure 4. ORTEP drawing of the molecular structure of II.

An analogous reaction of *hypho*- $\text{S}_2\text{B}_6\text{H}_9^-$ with diiodomethane resulted in the formation of a single product, which was found to be a carbadithiaborane containing a sulfur-bridging methylene group:



The ^{11}B NMR spectrum of III (Figure 5a) is strikingly similar to that of II, showing four doublets of relative intensities 2:2:1:1:

at similar chemical shifts, with the peak at -55.4 ppm again having additional triplet shifts, characteristic of coupling with two bridging hydrogens. The ^1H NMR spectrum shows, in addition to a bridging hydrogen resonance of intensity two at -0.66 ppm, two methylene proton resonances clearly split into a coupled AB pair ($J = 12$ Hz) at 1.78 and 1.47 ppm, respectively.

On the basis of skeletal electron counting procedures, III would be classified as a 9-vertex *hypho* cage system (26 skeletal electrons). As can be seen in the ORTEP drawing in Figure 6, a single-crystal X-ray determination confirmed that the compound has a geometry that is consistent with this prediction. The structure can be derived, as shown in Figure 7, from an icosahedron by the removal of three vertices.

The boron-boron and boron-sulfur distances in III are, as expected, quite similar to those observed for II; however, the B8 boron of the pentagonal boron ring is distorted (~ 0.25 Å) out of the plane of the remaining borons. The unique unbridged B10-B11 edge 1.64 (1) Å is within experimental error identical with that in II. The two bridging hydrogens, in agreement with both the NMR data obtained for III and the structure observed for II, are asymmetrically bound, being closer to B8 than to B7

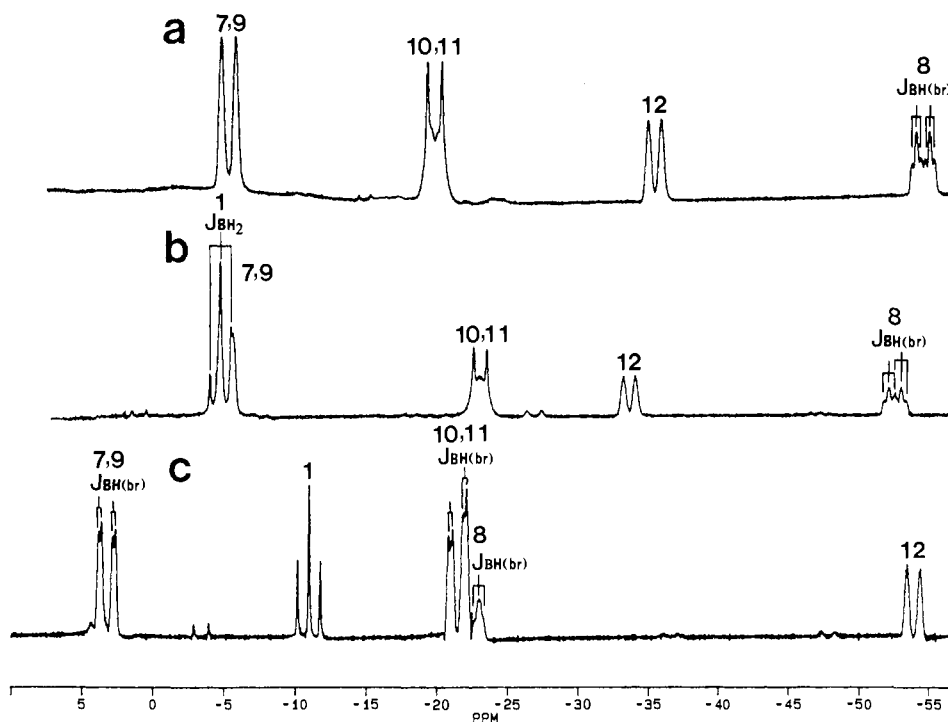


Figure 5. 160.5-MHz ^{11}B NMR spectra of III (a), IV (b), and V (c).

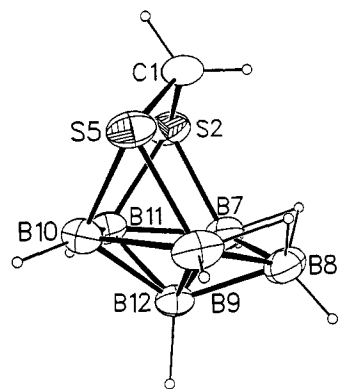


Figure 6. ORTEP drawing of the molecular structure of III.

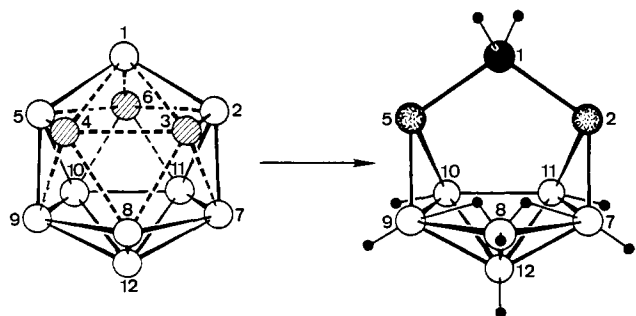


Figure 7. Derivation of a nine-vertex *hypho* structure for III from an icosahedron by removal of three vertices.

and B9. The nonbonded sulfur-sulfur distance 3.04 Å is somewhat shortened when compared to that in II, and as a result, the dihedral angles between the B9-B10-B11-B7 plane and the S5-B9-B10 (104°) and S2-B7-B11 (103°) planes are less than those in II.

Three previous examples of carbathiaboranes have been reported: $\text{SC}_2\text{B}_8\text{H}_{10}$,²³ 4,6,8- $\text{SC}_2\text{B}_6\text{H}_{10}$,²⁴ and 6,8- $\text{SCB}_7\text{H}_{11}$.¹⁶ The latter two compounds are isoelectronic and isostructural with *arachno*-6,8- $\text{S}_2\text{B}_7\text{H}_9$, with the carbon atoms present in both cases as CH_2 groups which, in contrast to the sulfur-bridging methylene observed in III, are bound to three borons in the cage framework. Boron-boron or boron-carbon bridging methylene groups have been previously observed as components of several carborane or metallacarborane cages. Structurally characterized examples include $\text{R}_2\text{C}_2\text{B}_{10}\text{H}_{11}^-$,²⁵ $\text{Cp}_2\text{Co}^+\text{Me}_4\text{C}_4\text{B}_8\text{H}_8^-$,²⁶ $\text{CpCoMe}_4\text{C}_4\text{B}_7\text{H}_7$,²⁷ and $\text{Me}_4\text{C}_4\text{B}_7\text{H}_9$.²⁸ It should also be noted that, while sulfur-sulfur bridging methylenes have not previously been observed in dithiaboranes, they are a common feature in metal-sulfur clusters, including compounds such as $\text{CH}_2\text{S}_2\text{Fe}_2(\text{CO})_6$,²⁹ $\text{CH}_2\text{S}_2(\text{CpMoS})_2$.³⁰

The methylene carbon in III is in a distorted tetrahedral environment, with the larger S2-C1-S5 angle 113.9 (3)° being necessitated by the presence of these three atoms in the planar pentagonal B10-B11-S5-C1-S2 ring. The C1-S2 and C1-S5 distances are comparable to those observed for the sulfur-methyl

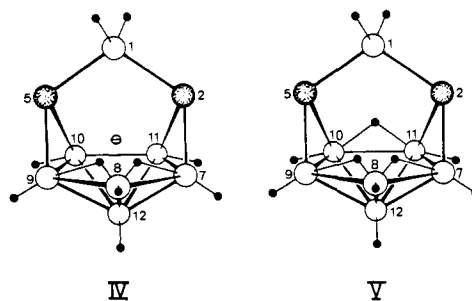
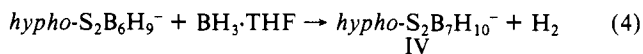


Figure 8. Proposed structures for IV and V.

distances observed in II, suggesting localized two-center two-electron bonding between the methylene unit and sulfur atoms.

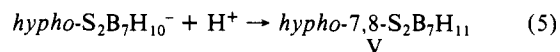
A wide range of 9-vertex *hypho* clusters in which the sulfur atoms are bridged by different species isoelectronic with a CH_2 unit, such as BH_2^- or BH_3 , should be possible. Shore³¹ has previously demonstrated that many polyhedral borane anions will readily add BH_3 to give expanded cage products (with or without loss of H_2) when reacted with diborane or BH_3 -ether adducts, and, indeed, it was found that reaction of the *hypho*- $\text{S}_2\text{B}_6\text{H}_9^-$ anion with $\text{BH}_3\cdot\text{THF}$ generated the boron analogue of III.



The composition of IV was established by elemental analysis of the PPN^+ salt. Since the compound is isoelectronic with III a similar structure is proposed, as shown in Figure 8.

The ^{11}B NMR spectrum (Figure 5b) of IV shows five resonances of relative intensities 1:2:2:1:1, with the bridging BH_2 group clearly indicated by the triplet resonance of intensity one at -5.8 ppm. The remainder of the spectrum is quite similar to those of II and III, indicating, as discussed earlier, the absence of a bridging hydrogen between B10 and B11. Also, in agreement with the proposed structure, the 200-MHz ^{11}B spin-decoupled ^1H NMR spectrum of IV shows only one type of bridge hydrogen and a coupled AB pair ($J = 8$ Hz) of resonances, which are attributed to the protons on the sulfur-bridging BH_2 unit.

Protonation of IV with gaseous HCl followed by vacuum-line fractionation resulted in the isolation of one product in high purity stopping in a -10 °C trap.



V was found to decompose slowly at room temperature but may be kept indefinitely under high vacuum at dry-ice temperature. The composition of V was established by exact mass measurements, and its proposed structure (Figure 8) is strongly supported by the NMR data. Thus, in the ^{11}B NMR spectrum (Figure 5c) the bridging - BH_2 group is clearly identified by the triplet resonance at -11.5 ppm, with the remainder of the spectrum being essentially identical with that of I. The 200-MHz ^{11}B spin-decoupled ^1H NMR spectrum of V shows resonances corresponding to the terminal -BH groups and two types of B-H-B bridge protons. Upon boron decoupling the bridging proton of intensity one at -0.47 ppm appears as a triplet ($J = 7.5$ Hz), owing to its coupling to two terminal hydrogens, and the two BH_2 protons again appear as a coupled AB pair at 2.56 and 1.45 ppm.

On the basis of the reaction observed between $\text{S}_2\text{B}_6\text{H}_9^-$ and $\text{BH}_3\cdot\text{THF}$ (eq 4), it was expected that the reaction of the *arachno*- $\text{S}_2\text{B}_7\text{H}_9^-$ anion with $\text{BH}_3\cdot\text{THF}$ might lead to the formation of a new 10-vertex *hypho* cage system such as $\text{S}_2\text{B}_8\text{H}_{11}^-$. Surprisingly, however, the reaction does not yield a 10-vertex system but instead gives *hypho*- $\text{S}_2\text{B}_7\text{H}_{11}^-$ (IV). Likewise, IV also results

(23) Brattsev, V. A.; Knyazev, S. P.; Danilova, G. N.; Stanko, V. I. *Zh. Obshch. Khim.* **1975**, *45*, 1393-1394.

(24) Baše, K.; Heřmánek, S.; Hanousek, F. *J. Chem. Soc., Chem. Commun.* **1984**, 299-300.

(25) (a) Dunks, G. B.; Wiersema, R. J.; Hawthorne, M. F. *J. Am. Chem. Soc.* **1973**, *95*, 3174-3179. (b) Tolpin, E. I.; Lipscomb, W. N. *Inorg. Chem.* **1973**, *12*, 2257-2262.

(26) Grimes, R. N.; Pipal, J. R.; Sinn, E. *J. Am. Chem. Soc.* **1979**, *101*, 4172-4180.

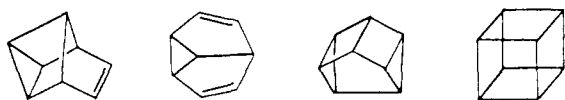
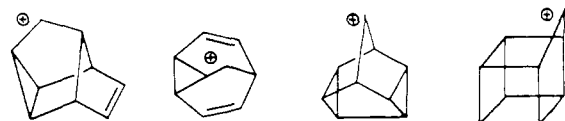
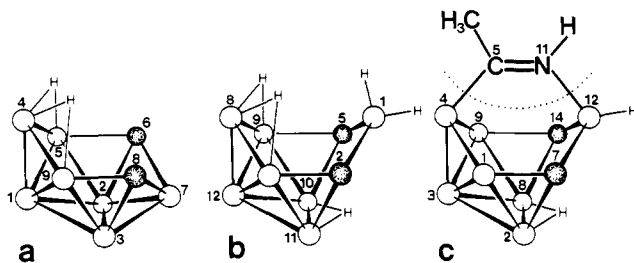
(27) Grimes, R. N.; Sinn, E.; Pipal, J. R. *J. Am. Chem. Soc.* **1980**, *102*, 2087-2095.

(28) Finster, D. C.; Grimes, R. N. *J. Am. Chem. Soc.* **1981**, *103*, 2675-2683.

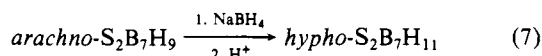
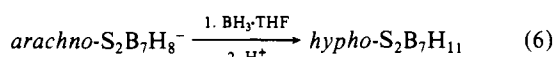
(29) Shaver, A.; Fitzpatrick, P. J.; Steliou, K.; Butler, I. S. *J. Am. Chem. Soc.* **1979**, *101*, 1313-1315.

(30) McKenna, M.; Wright, L. L.; Miller, D. T.; Tanner, L.; Haltiwanger, R. C.; DuBois, M. R. *J. Am. Chem. Soc.* **1983**, *105*, 5329-5337.

(31) (a) Johnson, H. D., II; Bruce, V. T.; Shore, S. G. *Inorg. Chem.* **1973**, *12*, 689. (b) Johnson, H. D., II; Shore, S. G. *J. Am. Chem. Soc.* **1971**, *93*, 3798-3799. (c) Geanangel, R. A.; Johnson, H. D., II; Shore, S. G. *Inorg. Chem.* **1971**, *10*, 2363-2364.

C_8H_8 Cage Structures $C_9H_9^+$ Cage StructuresFigure 9. Cage structures confirmed or proposed for C_8H_8 or $C_9H_9^+$.Figure 10. Comparison of the structures of *arachno*-6,8- $S_2B_7H_9$, *hypho*-7,8- $S_2B_7H_{11}$, and *hypho*-5- CH_3 -5,11,7,14- $CNS_2B_7H_8$.

from the direct reaction of *arachno*-6,8- $S_2B_7H_9$ with $NaBH_4$ in dioxane under reflux conditions.



These reactions are, in fact, more convenient synthetic routes to V than the pathway given in eq 4.

Discussion

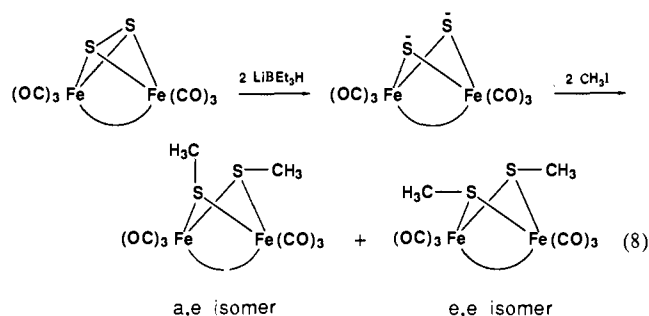
The series of new eight- (I and II) and nine-vertex (III–V) *hypho*-dithiaborane clusters discussed above are unprecedented in polyhedral borane chemistry; however, related cage compounds are well-known in both organic and transition-metal cluster chemistry.

For example, I and II are isoelectronic (in a cluster sense) with C_8H_8 , and III–V are isoelectronic analogues of the $C_9H_9^+$ carbocation. Several structures that have been either confirmed or proposed for organic cage fragments with the compositions of C_8H_8 or $C_9H_9^+$ are shown in Figure 9.³² Comparison of these structures with those determined for II (Figure 4) and III (Figure 6) reveal significant differences. Most importantly, the boron atoms in both II and III occupy either four- or five-coordinate positions in the cage, while the carbon atoms in either C_8H_8 and $C_9H_9^+$ are in only two- or three-coordinate cage positions. These differences most likely arise because of the hybrid nature of the dithiaborane clusters resulting in the localization of skeletal electrons between the more electronegative elements (carbon or sulfur). For example, in III the electron-rich bridging $S-CH_2-S$ unit appears to be connected by conventional two-center two-electron bonds, whereas the electron-deficient six-boron unit adopts a configuration that favors multicenter interactions. Thus, these molecules can be described as having both classical and nonclassical portions. Such a trend is also evident when the structures (parts a and b of Figure 10 of *arachno*-6,8- $S_2B_7H_9$ and *hypho*-7,8- $S_2B_7H_{11}$ are compared.

In *arachno*-6,8- $S_2B_7H_{11}$, boron B7 is bound to both sulfurs and borons B2 and B3 and is clearly part of the cage framework. In *hypho*-7,8- $S_2B_7H_{11}$, the tetrahedral boron B1 is attached to only the two sulfur atoms by what could be considered two-center two-electron interactions. It should also be noted that the cage framework in V is remarkably similar to that determined for the thiaborane fragment in the compound *hypho*-5- CH_3 -5,11,7,14- $CNS_2B_7H_8$ (Figure 10c), which, as we previously discussed,¹⁴ may be described either as an 11-vertex *hypho* cage system or a 9-vertex *hypho* cage with a bridging imine substituent.

The above observations suggest that in these systems the transition from an electron-deficient to electron-precise cluster occurs by the progressive formation of two-center bonds to produce classical components and, furthermore, bring into question at what point should such a classical fragment be considered as an exopolyhedral substituent rather than a component of a cluster framework. For example, even though an eight-vertex *hypho* formulation seems reasonable for I, the isoelectronic compound II might alternately be described as a six-vertex *nido* system substituted by "classical" methanethiol groups, i.e. *nido*-(μ -MeS) $_2B_6H_8$. Clearly, more structurally characterized examples of larger cage *hypho* clusters will be needed before the nature of the bonding interactions within these clusters can be fully understood.

The structure and reactivities of I and II may also be compared with other types of clusters, particular transition-metal sulfur complexes, containing bridging sulfur or methanethiol groups. For example, the anion $Fe_2(CO)_6S_2^{2-}$ can be readily generated from the complex $Fe_2(CO)_6S_2$ and has been found to react with methyl iodide as follows.³³



Methylation occurs exclusively at the sulfur atoms consistent with a localization of negative charge at these sites in the $Fe_2(CO)_6S_2^{2-}$ anion. Protonation of $Fe_2(CO)_6S_2^{2-}$ yields the corresponding thiol compounds $Fe_2(CO)_6(SH)_2$.³³ In contrast to these results, in *hypho*- $S_2B_6H_9^-$ (I; which would be the protonated analogue of the $S_2B_6H_8^{2-}$ anion), the additional proton is present not as a thiol, as found in $Fe_2(CO)_6(SH)_2$ but rather in a bridge site on the borane fragment. Furthermore, I will not react with additional acid to give the neutral compound $S_2B_6H_{10}$ but instead decomposes. On the other hand, I does react with 2 equiv of methyl iodide to give the dimethylated product in which alkylation has occurred exclusively at the sulfurs. Thus, the negative charge in I must be localized at the sulfur sites and initial methylation apparently increases the acidity of the unique bridging hydrogen so that reaction with an additional 1 equiv of methyl iodide is possible. Thus, I exhibits a reactivity that in many ways parallels that observed for $S_2Fe_2(CO)_6^{2-}$.

Likewise, the reaction of I with diiodomethane or $BH_3 \cdot THF$ to yield the nine-vertex bridged complexes III and IV was suggested by similar reactions observed in metal-sulfur cluster chemistry. For example, Seyferth³⁴ has observed that S_2Fe_2-

(32) Leone, R. E.; Barborak, J. C.; Schleyer, P. v. R. In *Carbonium Ions*; Olah, G. A., Schleyer, P. v. R., Eds.; Wiley: New York, 1973; pp 1837–1939 and references therein.

(33) Seyferth, D.; Henderson, R. S.; Song, L.-C. *J. Organomet. Chem.* **1980**, *192*, C1–C5.

(34) Seyferth, D.; Henderson, R. S.; Song, L.-C. *Organometallics* **1982**, *1*, 125–133.

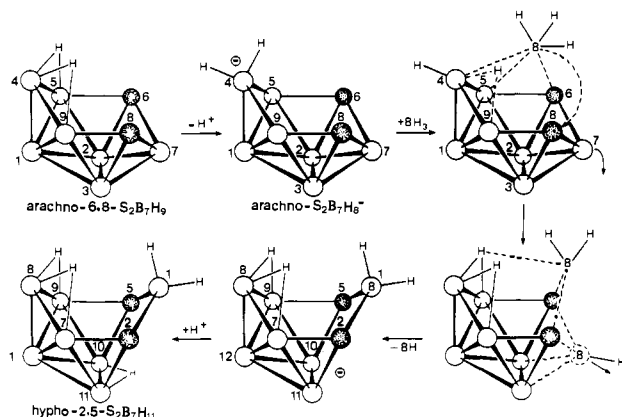
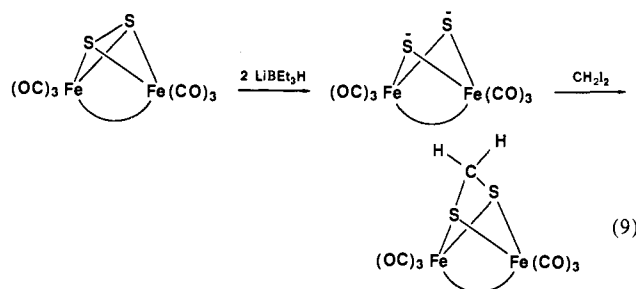


Figure 11. Possible reaction sequence leading to the formation of V from the reaction of *arachno*- $S_2B_7H_8^-$ with $BH_3 \cdot THF$.

$(CO)_6^{2-}$ will react with diiodomethane to generate the methylene-bridged compound shown below:

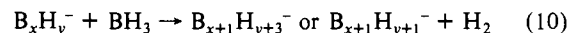


Numerous other bridged derivatives of $S_2Fe_2(CO)_6^{2-}$ have also been generated³⁴ by reaction of the anion with various dihalides, and it is now expected that comparable reactions with I will result in the production of a wide variety of new nine-vertex *hypho* clusters. Furthermore, because of the hybrid nature of these new clusters, they may well exhibit structural and bonding patterns not encountered in conventional polyhedral boranes and metal cluster systems.

Finally, the initial steps involved in the reactions (eq 1, 6, and 7) resulting in the direct formation of I, IV, or V from *arachno*- $6,8-S_2B_7H_9$ are deserving of special comment, because of the unique reactivity exhibited by the B7 boron in the *arachno*- $6,8-S_2B_7H_9$ framework (Figure 10a). Since B7 sits between the two electronegative sulfur atoms, it is apparently activated for

attack by nucleophiles, and either rearrangement or cleavage reactions can result. For example, we previously proposed that the formation of *hypho*- $5-CH_3-5,11,7,14-CNS_2B_7H_8$ in the reaction of *arachno*- $S_2B_7H_8^-$ with acetonitrile may involve an initial nucleophilic attack of the anion at the nitrile carbon, followed by a cage condensation rearrangement that is driven by the formation of a dative bond between the imine lone pair and the electropositive B7 boron atom. The formation of the *hypho*- $S_2B_6H_9^-$ anion may occur in an analogous sequence involving nucleophilic attack of *arachno*- $S_2B_7H_8^-$ at the electropositive acetone carbon, followed by attack of the oxygen at the B7 boron position ultimately leading to framework degradation and generation of the six-boron anion.

The formation of *hypho*- $7,8-S_2B_7H_{11}$ (V) from the reactions of *arachno*- $S_2B_7H_9$ with either $BH_3 \cdot THF$ or $NaBH_4$ was quite unexpected, since it is well established³¹ that many borane anions will react with diborane or BH_3 -adducts to generate higher boron clusters:



Such reactions may be viewed as involving an initial interaction between the Lewis acid BH_3 and the basic borane anion, followed by a cluster condensation. The formation of V, rather than either $S_2B_8H_{11}$ or $S_2B_8H_9$, in the reactions given in eq 6 and 7 may arise because of the unique reactivity of the B7 boron in *arachno*- $6,8-S_2B_7H_9$. A possible reaction sequence leading to the formation of IV and V is shown in Figure 11. Thus, a BH_3 unit should initially add to the anion at the B4-B5-S6 edge to produce an unstable $S_2B_8H_{12}^-$ intermediate. In view of the cage rearrangement and degradation reactions involving B7, which were discussed above, a weakening of the cage bonding interaction with B7 might again be expected, resulting in decomposition of the framework by cleavage of this boron. This proposed reaction sequence is entirely speculative and additional detailed studies will be required before an exact reaction mechanism can be confirmed; however, it is clear that the B7 boron appears to play a unique role in each of the reactions discussed above.

Acknowledgment. We thank the National Science Foundation for the support of this research. We also thank Dr. Robert Williams for his comments and Dr. Pat Carroll for his assistance in the X-ray crystallographic studies.

Supplementary Material Available: Tables of anisotropic temperature factors, hydrogen atom coordinates, bond angles, and least-squares planes (9 pages); listings of observed and calculated structure factor amplitudes (6 pages). Ordering information is given on any current masthead page.